European Journal of Nuclear Medicine and Molecular Imaging (2019) 46:2042–2050
https://doi.org/10.1007/s00259-019-04415-3

ORIGINAL ARTICLE

Prospective diagnostic performance of semiconductor SPECT myocardial perfusion imaging: wall thickening analysis reduces the need for an additional prone acquisition

Loïc Djaileb[1,2,3] · Benjamin Dubois[4] · Nicolas de Leiris[1,3] · Julien Leenhardt[1,3] · Marjorie Canu[1] · Olivier Phan Sy[3] · Adrien Carabelli[1,5] · Bastien Boussat[6] · Laurent Dumas[1,2] · Alexis Broisat[1,2] · Gérald Vanzetto[1,2,5] · Daniel Fagret[1,2,3] · Catherine Ghezzi[1,2] · Gilles Barone-Rochette[1,2,5] · Laurent M. Riou[1,2]

Received: 5 February 2019 / Accepted: 25 June 2019 / Published online: 18 July 2019

Abstract

Purpose To determine whether the assessment of regional wall thickening (WT) in addition to myocardial perfusion from stress supine acquisitions could compensate for the lack of prone acquisition and the corresponding decrease in the diagnostic performance of SPECT myocardial perfusion imaging (MPI) in patients with known or suspected coronary artery disease (CAD).

Methods The study group comprised 41 patients (123 vessels) with known or suspected CAD prospectively recruited for systematic prone and supine ^{201}Tl stress SPECT MPI. The diagnostic performance of SPECT MPI was determined for various image sets including nongated supine images (supine NG), nongated combined prone and supine images (prone and supine NG) and gated supine images, allowing WT evaluation from NG images in addition to perfusion (supine NG + WT) using invasive coronary angiography and fractional flow reserve as the gold standards.

Results The rate of false positives was significantly higher among the supine NG images (20.8%) than among either the prone and supine NG or the supine NG + WT images (3.3% and 2.7%, respectively, $P < 0.05$ vs. supine NG). Consequently, specificity was higher for the prone and supine NG images than for the supine NG images (96.1% vs. 76.1%, $P < 0.01$) and was highest for the supine NG + WT images (96.8%, P not significant vs. prone and supine NG), without significant differences in sensitivity (80.0%, 86.6% and 73.3%, respectively, P not significant for all comparisons).

Conclusion The diagnostic performance of supine stress SPECT MPI is improved when WT assessment of ischaemic segments is used as an additional diagnostic criterion to values not significantly different from those with combined prone and supine acquisitions.

Keywords SPECT · CZT · Coronarography · FFR · Wall thickening · Diagnostic performance

This article is part of the Topical Collection on Cardiology

Electronic supplementary material The online version of this article (https://doi.org/10.1007/s00259-019-04415-3) contains supplementary material, which is available to authorized users.

✉ Laurent M. Riou
Laurent.Riou@univ-grenoble-alpes.fr

[1] INSERM, U1039, Radiopharmaceutiques Biocliniques, Faculté de Médecine de Grenoble, F-38700 La Tronche, France

[2] Université Grenoble-Alpes, Grenoble-Alpes, France

[3] Nuclear Medicine Department, Grenoble-Alpes University Hospital, Grenoble-Alpes, France

[4] Nuclear Medicine Department, Savoie Metropole Hospital, Chambery, France

[5] Cardiology Department, Grenoble-Alpes University Hospital, Grenoble-Alpes, France

[6] TIMC-IMAG, UMR CNRS 5525, Grenoble-Alpes, France

Introduction

The use of combined prone and supine image acquisition for single-photon emission computed tomography (SPECT) myocardial perfusion imaging (MPI) has been shown to: (1) improve interobserver agreement [1], (2) decrease the rate of occurrence of equivocal studies by limiting the influence of artefacts originating from supine-only acquisitions, [2–4], thereby (3) improving specificity without compromising sensitivity in a wide range of patient populations [2, 5, 6], and (4) improve prognostic accuracy [7]. These findings have recently been observed with cardiac-dedicated cadmium zinc telluride (CZT) cameras [8, 9] and have been attributed to the specific artefacts generated by this equipment [10–12]. However, despite their clinical relevance, the use of prone acquisitions either instead of or in combination with supine acquisitions remains very limited, with only 16% of studies from European centres being performed using such procedures as of 2007 [13]. The limited use of combined prone and supine acquisitions has been suggested to be mainly related to poor patient tolerance of the prone position [3] due to physical limitations in up to 20% of cases [2], while the historical argument of workflow impediment due to the increased time required for image acquisition has been weakened by the recent introduction of CZT cameras that have higher sensitivity and therefore shorter acquisition times [14]. The procedure of ECG gating has gained much wider clinical acceptance than performing prone acquisitions, with 74% of perfusion studies in Europe being ECG-gated [13]. ECG-gated SPECT acquisitions allow the assessment of global and regional left ventricular (LV) function [15, 16]. When combined with perfusion, the additional regional functional data significantly reduces the number of borderline normal or abnormal readings, thereby decreasing the false-positive rate and improving test specificity [17–21].

Recently introduced cardiac-dedicated semiconductor SPECT cameras display improved sensitivity and resolution compared with Anger cameras and therefore provide more accurate functional image analysis [22]. The feasibility of regional functional assessment in addition to perfusion using new-generation semiconductor cameras has recently been demonstrated in comparison with alternative imaging modalities [23]. However, few data are available regarding the clinical relevance of regional functional assessment from images acquired using CZT cameras with regard to the sensitivity and specificity values of SPECT MPI [14]. The aim of the present study was to determine whether the assessment of stress regional wall thickening (WT) in addition to myocardial perfusion from supine acquisitions could compensate for the lack of prone acquisition and the corresponding decrease in diagnostic performance of SPECT MPI in patients with known or suspected coronary artery disease (CAD).

Materials and methods

The study (EVACORY, NCT01995955) was approved by the Comité de Protection des Personnes (CPP) SUD EST V Ethics Committee, and all subjects gave written informed consent to participate.

Study population

A total of 55 patients with known or suspected CAD were prospectively recruited in the framework of an ancillary study (main study, EVACORY, NCT01995955) between June 2013 and October 2016. The patients had systematic SPECT MPI and invasive coronary angiography (ICA) including assessment of fractional flow reserve (FFR) irrespective of the results of the noninvasive scintigraphic assessment of myocardial perfusion. Of the 55 patients, 41 underwent both prone and supine stress acquisitions and were included in the present study.

Exclusion criteria were as follows: previous ST segment elevation or non-ST segment elevation myocardial infarction, haemodynamic instability, significant valvular disease stenosis, coronary artery bypass grafting, nonischaemic cardiomyopathy, severely reduced LV ejection fraction (≤35%), and contraindications to adenosine stress. Contraindications to adenosine were asthma, second- or third-degree atrioventricular block or sick sinus syndrome without a pacemaker, systolic blood pressure less than 90 mmHg, dipyridamole-containing medication, methyl xanthene medication within 12 h of the test, and known hypersensitivity to adenosine.

Stress protocols

Stress testing was performed as previously described [24]. Details are provided in Online Resource 1.

Imaging protocol

The imaging protocol is depicted in Fig. 1 with further details being provided in Online Resource 1.

Analysis of perfusion images

The image analysis procedure used in the present study is summarized in Fig. 2. Non-ECG-gated (NG) images, ECG-gated end-systolic (ES) images, and ECG-gated images for regional WT analysis obtained in each patient from both the prone and supine acquisitions were allocated to nine image sets by an independent observer (B.D.) to assess the diagnostic performance of SPECT MPI using the following image combinations: *set 1* prone NG images, *set 2* supine NG images, *set 3* prone and supine NG images, *set 4* prone NG + WT images;, *set 5* supine NG + WT supine images, *set 6* prone and supine

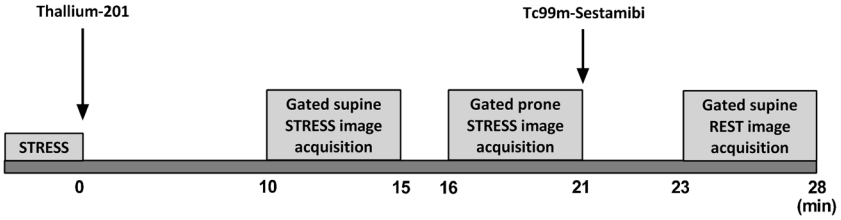

Fig. 1 Imaging protocol. Stress testing was performed using either an ergometer or dipyridamole. Patients were injected with ^{201}Tl at peak stress. Supine and prone images were acquired sequentially each over 5 min starting 10 min after ^{201}Tl injection. ^{99m}Tc-sestamibi was injected upon completion of the prone stress image acquisition and a 5-min rest image was acquired 2 min later

NG + WT images, *set 7* prone ES images, *set 8* supine ES images, and *set 9* prone and supine ES images.

For each image set, stress and rest myocardial perfusion was semiquantitatively evaluated by visual scoring using a five-point scale (*0* normal radiotracer uptake, *1* equivocal uptake, *2* moderate uptake , *4* severely reduced uptake, *4* no detectable uptake) and a 17-segment model of the LV [25]. Semiquantitative perfusion scoring was performed by two experienced nuclear cardiologists (L.D., D.F.). Global summed stress scores (SSS) and summed rest scores (SRS) were calculated by adding the scores of all 17 segments from stress or rest images. Coronary territory perfusion was calculated after allocating the 17 segments to the left anterior descending coronary artery (LAD), left circumflex coronary artery (LCx) or right coronary artery (RCA) territory as described below. Per-segment myocardial perfusion was considered pathological when there was a reversible (SSS ≥2 and SRS ≤2) or fixed (necrosis, SSS and SRS both ≥2) perfusion defect. The extent of ischaemia (LV percentage) was determined by dividing the number of ischaemic segments (SSS ≥2 and SRS ≤2) by the total number of LV segments. WT was evaluated visually by experienced nuclear cardiologists (L.D., B.D.) in each of the 17 myocardial segments based on the increase in brightness of the LV wall over the cardiac cycle. WT was scored on a five-point scale (*0* normal, *1* mildly impaired, *2* moderately impaired, *3* severely impaired, *4* absent) and was eventually considered as normal (WT score 0) or abnormal (WT score ≥1) based on myocardial wall brightening from diastole to systole [16, 26] and by comparison with segments from the same myocardial slice.

Two experienced nuclear cardiologists (L.D., D.F.) performed the semiquantitative perfusion analysis of each

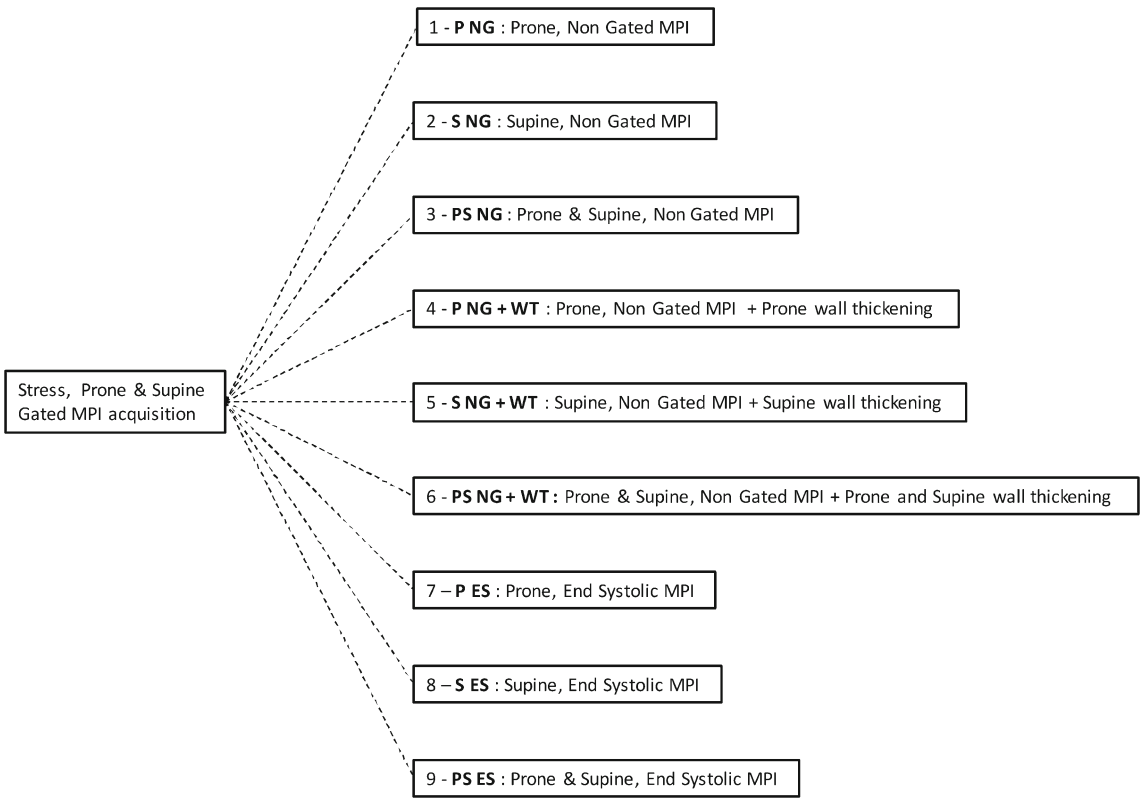

Fig. 2 Image sets used in the present study. Results from ES images (sets 7, 8, and 9) are presented and discussed in Online Resource 1

image set blinded to the ICA data and to the perfusion scores of other image sets. Discordant findings were resolved by consensus. Per-patient and per-coronary territory myocardial perfusion was considered pathological when the extent of ischaemia was >10% LV or when necrosis (segmental SSS and SRS >2) was present in at least one segment on prone or supine images (sets 1 and 2). For image set 3 in which both prone and supine images were considered, segmental myocardial perfusion was considered pathological when both prone and supine images indicated a similar segmental perfusion abnormality, in which situation the lowest score was retained to minimize the occurrence of perfusion artefacts. A similar procedure was used for the analysis of myocardial perfusion on ES images (sets 7, 8 and 9). Finally, WT analysis in addition to NG perfusion images (sets 4, 5 and 6) was used to classify myocardial perfusion as pathological when a myocardial segment with SSS ≥2 also showed a WT abnormality. When both prone and supine acquisitions were used for WT analysis (set 6), a WT abnormality was considered present only if observed on both images.

Invasive coronary angiography

ICA was performed and selective FFR determined using standard techniques (Allura Xper FD10; Philips Healthcare) as detailed in Online resource 1. The association between the 17-myocardial segment model and the actual coronary anatomy was determined as previously described [27]. Accordingly, segments 1, 2, 7, 8, 13, 14, 16 and 17 were attributed to the LAD and segment 6 to the LCx irrespective of coronary dominance. If positive on perfusion analysis, the remaining segments were attributed to the coronary territory which was abnormal on coronarography (segments 3, 9 and 15 to the LAD or RCA; segments 4, 5, 10 and 11 to the RCA or LCx; and segment 12 to the LAD or LCx).

Statistical methods

Statistical analyses were performed using SPSS® version 15.0 (SPSS Inc., Chicago, IL). Continuous and discrete (SSS and SRS) variables are expressed as means ± standard deviation. Sensitivity, specificity, positive predictive value, negative predictive value and accuracy were calculated for MPI with respect to CAD detection. Interobserver and intraobserver reliability for SSS and SRS scores were assessed using two-way random single-measure intraclass correlation coefficient analysis. SSS and SRS values found for the various image sets were compared using the Friedman test for paired nonparametric data with Dunn's post-hoc pair-wise multiple comparisons test. Sensitivity and specificity values were compared using the McNemar chi-squared test for paired categorical variables. P values <0.05 were considered to indicate statistical significance.

Results

Patient characteristics

The main patient characteristics are presented in Table 1. The 41 patients included in the study (66% men, age 62 ± 12 years) had a mean body mass index of 29.7 ± 5.9 kg/m^2, were predominantly referred for the detection of silent ischaemia (59%), and were predominantly (73%) classified as intermediate risk according to the European Society of Cardiology CAD consortium pretest probability of CAD clinical score, with none being classified as high risk. The most frequently observed cardiovascular risk factors were high blood pressure

Table 1 Study population characteristics

Characteristic	Value
Number of patients	41
Age (years), mean ± SD	62 ± 12
Sex (male), mean (SD)	27 (65.9)
Body mass index (kg/m^2), mean ± SD	29.7 ± 5.9
Hypertension, *n* (%)	27 (65.8)
Dyslipidaemia, *n* (%)	23 (56)
Diabetes mellitus, *n* (%)	23 (56)
Current smoker, *n* (%)	13 (31.8)
Family history of CAD, *n* (%)	5 (12.2)
CAD history, *n* (%)	9 (22)
Previous stroke, *n* (%)	3 (7.3)
Treatment, *n* (%)	
Antiplatelet	23 (56.1)
Beta-blockers	19 (46.3)
Calcium inhibitors	8 (19.5)
ACE inhibitors	8 (19.5)
ARBs	15 (36.6)
Diuretics	12 (29.2)
Statins	26 (63.4)
Indication for testing, *n* (%)	
Typical chest pain	6 (14.6)
Atypical chest pain	11 (26.8)
Silent ischaemia detection, *n* (%)	24 (58.5)
Stressor	
Exercise	17 (41.5)
Dipyridamole	24 (58.5)
Dobutamine	0 (0)
Stress test results	
Maximum HR (bpm), mean ± SD	137.2 ± 14.0
Maximum HR (% MPHR), mean ± SD	88 ± 6
Positive, *n* (%)	4 (10)
Negative, *n* (%)	37 (90)

ACE angiotensin-converting enzyme, *ARBs* angiotensin-receptor blockers, *HR* heart rate, *MPHR* maximum predicted heart rate

(66%), dyslipidaemia (56%) and diabetes (56%). Of the 41 patients, 22% had known CAD and 15% had typical chest pain, and 17 (42%) underwent an exercise stress test while the remainder underwent pharmacological stress using dipyridamole. Gated acquisitions did not reach the required quality standards in two patients for either the prone or the supine acquisition, and in two patients for both the prone and the supine acquisitions.

Coronarography data

The results are presented in Table 2. In the 41 patients, 123 vessels were analysed, with FFR being assessed in 59 vessels (1.5 ± 0.8 vessels per patient). The prevalence of significant coronary stenosis was 29%. Of the 41 patients, 9 (22%) had single-vessel disease while 3 (7%) had double-vessel disease. The LAD, RCA and LCx were occluded in eight patients (53%), six patients (40%) and one patient (7%), respectively. Among the 123 epicardial vessels assessed, 15 (12%) had a significant coronary lesion (>50% stenosis). Of these 15 lesions, 10 (66%) had ≥90% stenosis, 4 (27%) were totally occluded, and 5 (33%) had 50–90% stenosis and a positive (<0.80) FFR value.

Table 2 Lesion characteristics

Variable	Value
Patients with significant coronary stenosis, *n* (% of 41 patients)	12 (29)
Significant coronary stenoses, *n* (% of 123 vessels)	15 (12)
Lesion location, *n* (% of 15 vessels with stenosis)	
LM	0 (0)
LAD	8 (53)
LCx	1 (7)
RCA	6 (40)
Number of vessels with significant lesions per patient, *n* (% of 41 patients)	
One vessel	9 (22)
Two vessels	3 (7)
Three vessels	0
Vessels with >90% stenosis, *n* (% of 15 vessels with stenosis)	10 (66)
Vessels with 100% stenosis, *n* (% of 15 vessels with stenosis)	4 (27)
Vessels with 50–90% stenosis and FFR <0.80, *n* (% of 15 vessels with stenosis)	5 (33)
Vessels with FFR evaluation	59 (47)
FFR, mean ± SD	
Vessels with FFR <0.80	0.60 ± 0.18
Vessels with FFR ≥0.80	0.90 ± 0.06
FFR-negative vessels, *n* (% of 59 vessels with FFR evaluation)	44 (75)
FFR-positive vessels, *n* (% of 59 vessels with FFR evaluation)	15 (25)
Stenosis (%), mean ± SD	
Vessels with FFR ≥0.80	21.4 ± 20.4
Vessels with FFR <0.80	77.3 ± 23.7

LM left main coronary artery, *LAD* left anterior descending coronary artery, *LCx* left circumflex coronary artery, *RCA* right coronary artery, *FFR* fractional flow reserve

Comparison of the extent and amplitude of myocardial ischaemia

The SSS values obtained from the prone NG and supine NG image sets (7.6 ± 6.0 and 7.6 ± 5.3, respectively) were significantly higher than those obtained from the prone and supine NG image set (3.6 ± 3.3; $P < 0.001$ for both comparisons).

Diagnostic performance

The diagnostic performance of each image set (sets 1–6) is presented in Table 3 and Fig. 3, and representative examples of image set 3 (prone and supine NG), set 2 (supine NG) and set 5 (supine NG + WT) from two patients are presented in Fig. 4. No significant differences were observed between the diagnostic performance of the prone NG and supine NG image sets. The specificity for the detection of significant CAD obtained from the prone and supine NG set (set 3; 96.1%, 95% CI 92–99%) was significantly higher than those obtained from either the prone NG set (set 1; 69.5%, 95% CI 60–78%, $P < 0.01$) or the supine NG set (set 2; 76.1%, 95% CI 68–84%, $P < 0.01$) with no significant differences in sensitivity values (set 3, 80%, 95% CI 59–100%; set 1, 86.6%, 95% CI 69–100%; set 2, 96.6%, 95% CI 69–100%).

Analysis of segmental WT in addition to supine NG images (set 5, supine NG + WT) significantly enhanced the specificity values of SPECT MPI compared with the values obtained using supine NG images alone (set 2; 96.8%, 95% CI 93–100%, vs. 76.1%, 95% CI 68–84%, respectively, $P < 0.01$) without significantly affecting sensitivity (73.3%, 95% CI 50–95%, with respect to the supine NG set 2 or prone and supine NG set 3 images; 86.6%, 95% CI 69–100%, and 80.0%, 95% CI 59–100%, *P* not significant). Overall, there was no significant difference in diagnostic performance between the prone and supine NG images and the supine NG + WT images. Similar trends were observed using prone images alone (Table 3). As detailed in Online Resource 1, the results obtained from analysis of WT in addition to supine NG images were not significantly improved by the use of ES images instead of conventional NG perfusion images (supplemental Figure). In addition, intraobserver reproducibility was high and equivalent for all tested combinations of SPECT and gated SPECT images (supplemental Table).

Table 3 Per-vessel diagnostic performance of image sets for the detection of significant coronary lesions

	Image set					
	Prone NG (set 1)	Prone NG + WT (set 4)	Supine NG (set 2)	Supine NG + WT (set 5)	Prone and supine NG (set 3)	Prone and supine NG + WT (set 6)
Number of vessels						
Total	120	111	120	111	120	114
True-positive	13	12	13	11	12	12
True-negative	73	93	80	93	101	99
False-positive	32	3	25	3	4	0
False-negative	2	3	2	4	3	3
Diagnostic accuracy (%)[a]	71.6 (63–80)	94.5 (89–98)	77.5 (69–85)	93.6 (87–97)	94.1 (88–98)	97.3 (93–99)
Sensitivity (%)	86.6 (69–100)	80.0 (59–100)	86.6 (69–100)	73.3 (50–95)	80.0 (59–100)	80.0 (59–100)
Specificity (%)	69.5 (60–78)	96.8 (93–100)	76.1 (68–84)	*96.8* (93–100)	**96.1** (92–99)	100
Positive predictive value (%)	28.8 (15–42)	80.0 (59–100)	34.2 (19–49)	78.5 (57–100)	75.0 (53–69)	100
Negative predictive value (%)	97.3 (93–100)	96.8 (93–100)	97.5 (94–100)	95.8 (91–99)	97.1 (93–100)	97.0 (93–100)

Values in parentheses are 95% confidence intervals

The value in italics is significantly different from the value for the Supine NG set at $P < 0.01$; the value in boldface is significantly different from the values for both the Supine NG set and the Prone NG set at $P < 0.01$

[a] Ratio of true-positive plus true-negative tests to the total number of tests

Discussion

The main finding of the present study is that the visual assessment of WT from SPECT stress myocardial perfusion images acquired in the supine position using a CZT detector camera compensated for the decrease in specificity for the detection of CAD caused by the lack of a prone acquisition by improving specificity values to levels not significantly different from those observed using combined prone and supine acquisitions without a significant decrease in sensitivity.

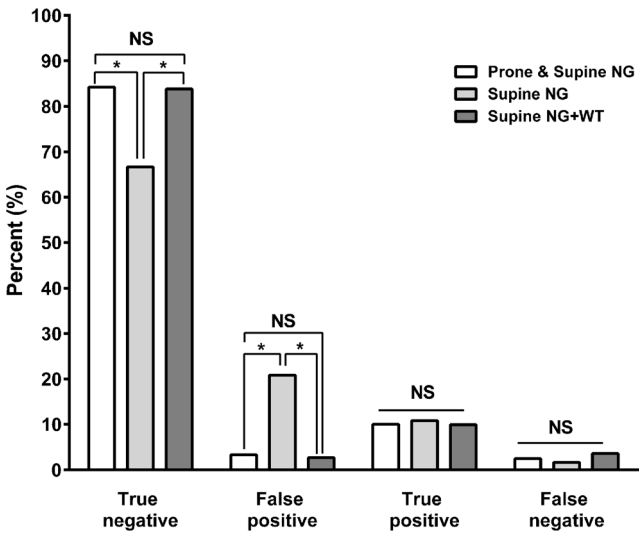

Fig. 3 True-negative, false-positive, true-positive and false-negative rates from the prone and supine NG image set, the supine NG set, and the supine NG + WT set. *$P < 0.05$; *NS* not statistically significant

The use of combined prone and supine acquisitions has been demonstrated to provide superior diagnostic and prognostic performance compared with prone-only or supine-only SPECT MPI, with both historical Anger cameras [2, 5–7] and recently developed CZT cameras [8, 9]. The present prospective study confirmed the excellent diagnostic performance of CZT SPECT MPI for the detection of significant coronary stenosis assessed by ICA and FFR when both prone and supine images were acquired, in accordance with the previously published data discussed above. An alternative to the acquisition of both prone and supine images is the use of ECG-gated imaging for the evaluation of regional cardiac function through the assessment of systolic WT. Accordingly, a number of studies have validated the hypothesis that the diagnostic performance of SPECT MPI is improved when it is combined with regional function assessment on Anger cameras [18–22]. However, the increased spatial resolution provided by recently available CZT cameras leads to a corresponding decrease in partial volume loss that may lead to underestimation of myocardial WT based on the partial volume effect, although this issue does not yet appear to have been conclusively addressed [22, 23, 28].

In addition, there are few data in the recent literature addressing the potential of CZT cameras for the assessment of systolic WT [29, 30]. In this setting, the results of the present

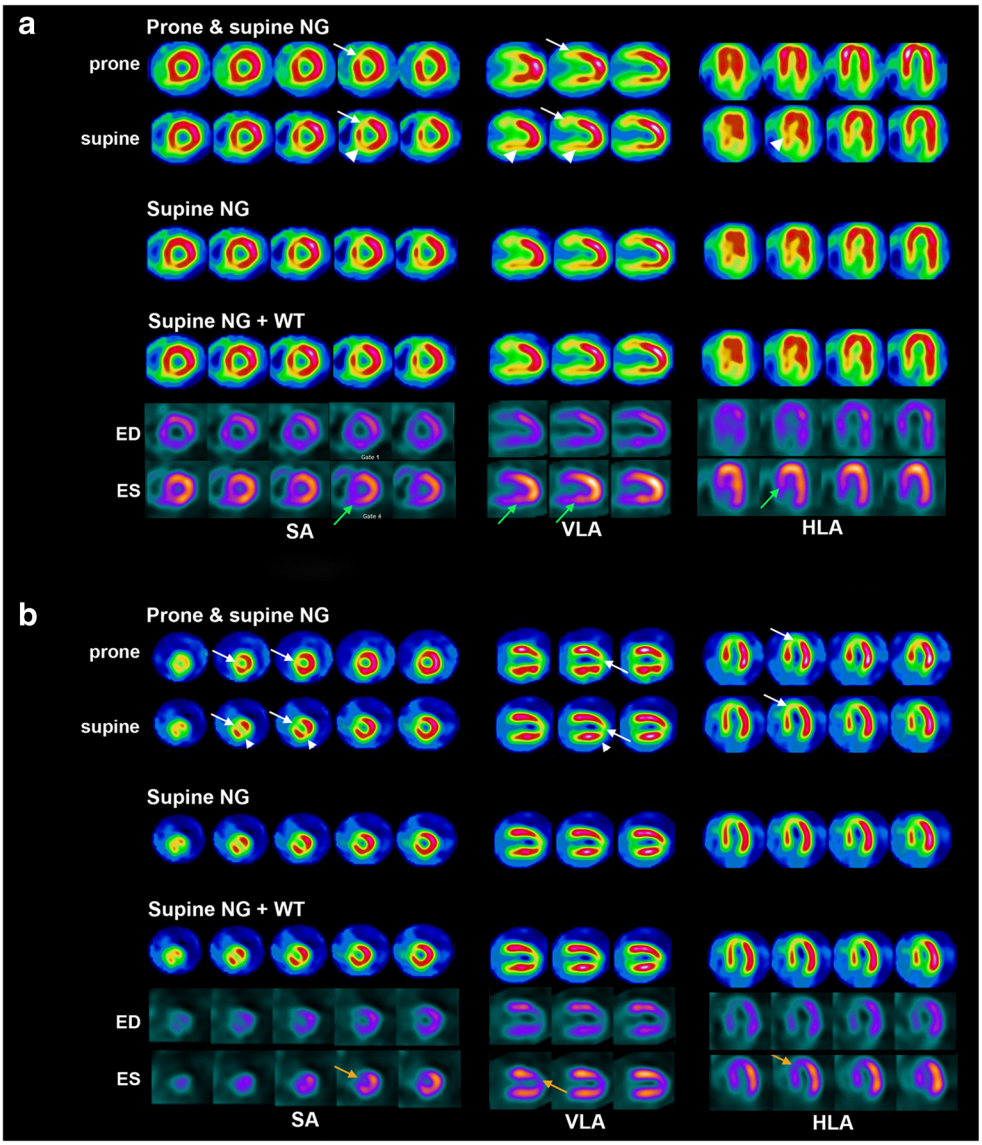

Fig. 4 Representative examples of Prone and supine NG, Supine NG, and Supine NG + WT image sets. **a** The Prone and supine NG images show <5% ischaemia (SSS = 2) which increases to 10–15% on the Supine NG images (SSS = 6); WT analysis of the supine images (Supine NG + WT images) indicates no wall thickening abnormality, confirming the lack of ischaemia found on analysis of the Prone and supine NG images. The coronarography data indicated no significant CAD (LAD, 20% stenosis; LCx, 0% stenosis; RCA, 20% stenosis). Rest images (Supine NG + WT images) are normal; **b** The Prone and supine NG images show 10–15% anterior ischaemia (SSS = 5) which increases to 15–20% on the Supine NG images (SSS = 9); WT analysis of supine images (Supine NG + WT images) indicates a thickening abnormality confirming the presence of ischaemia. The coronarography data indicated significant LAD stenosis (70%, FFR 0.79) while the LCx (60% stenosis, FFR 0.93) and RCA (30% stenosis) did not display significant CAD. Rest images (Supine NG + WT images) are normal. *White arrows* myocardial perfusion defects on both the prone and supine acquisitions, *arrowheads* supine-specific myocardial perfusion defects, *green arrows* areas of normal wall thickening despite supine-specific myocardial perfusion defects indicating the artefactual nature of the perfusion abnormality, *orange arrows* areas of impaired wall thickening in the ischaemic area; *SA* short axis, *VLA* vertical long axis, *HLA* horizontal long axis

study seem to indicate the relevance of visual assessment of regional WT based on the variation in myocardial intensity over the cardiac cycle since the combination of perfusion analysis from NG supine or prone images combined with the assessment of regional WT on the same acquisitions allowed improvement in specificity to values not significantly different from those obtained using the combination prone and supine NG perfusion images. With respect to the reliability of specificity values found in this study, it should also be noted that post-test referral bias was absent since all included patients underwent ICA irrespective of the presence or absence of myocardial ischaemia from SPECT MPI. As a result, the diagnostic performance of the various image sets used in this study was determined in a cohort in which a significant proportion of coronary angiograms were negative for CAD, thereby avoiding the need to use normalcy rate [31, 32].

Study limitations

The present study was a single-centre study with a relatively low sample size, and this may have limited its statistical power. However, the relatively small number of patients included was a consequence of the prospective design of the trial, and because of this there was no referral bias and ICA and FFR assessment were performed systematically. The relatively high doses of ^{201}Tl and ^{99m}Tc-sestamibi injected were chosen as previously described by others [33]. The corresponding effective dose may be optimized through stress-only acquisitions and minimization of the injected activity of ^{201}Tl, as currently performed and evaluated in our institution.

Conclusion

CZT SPECT MPI showed excellent performance for the detection of significant coronary stenosis as identified by ICA and FFR when both prone and supine acquisitions can be performed. Specificity is impaired when supine-only acquisitions are available. In this setting, the visual analysis of segmental WT on ECG-gated images and the use of the composite criterion for myocardial ischaemia of >10% LV and WT abnormality in the corresponding ischaemic segments for the classification of a CZT SPECT MPI test as positive significantly improves the diagnostic performance of supine-only acquisitions.

Acknowledgements The authors are grateful to Alexandre Seiller for expert assistance with the statistical analysis.

Compliance with ethical standards

Conflicts of interest None.

Ethical approval All procedures performed in studies involving human participants were in accordance with the ethical standards of the institutional and/or national research committee and with the principles of the 1964 Declaration of Helsinki and its later amendments or comparable ethical standards.

Informed consent Informed consent was obtained from all individual participants included in the study.

References

1. Arsanjani R, Hayes SW, Fish M, Shalev A, Nakanishi R, Thomson LE, et al. Two-position supine/prone myocardial perfusion SPECT (MPS) imaging improves visual inter-observer correlation and agreement. J Nucl Cardiol. 2014;21:703–11.
2. Taasan V, Wokhlu A, Taasan MV, Dusaj RS, Mehta A, Kraft S, et al. Comparative accuracy of supine-only and combined supine-prone myocardial perfusion imaging in men. J Nucl Cardiol. 2016;23:1470–6.
3. Malkerneker D, Brenner R, Martin W, Sampson U, Feurer I, Kronenberg M, et al. CT-based attenuation correction versus prone imaging to decrease equivocal interpretations of rest/stress Tc-99m tetrofosmin SPECT MPI. J Nucl Cardiol. 2007;14:314–23.
4. Segall GM, Davis MJ, Goris ML. Improved specificity of prone versus supine thallium SPECT imaging. Clin Nucl Med. 1988;13:915–6.
5. Slomka P, Nishina H, Abidov A, Hayes S, Friedman J, Berman D, et al. Combined quantitative supine-prone myocardial perfusion SPECT improves detection of coronary artery disease and normalcy rates in women. J Nucl Cardiol. 2007;14:44–52.
6. Berman D, Kang X, Nishina H, Slomka P, Shaw L, Hayes S, et al. Diagnostic accuracy of gated Tc-99m sestamibi stress myocardial perfusion SPECT with combined supine and prone acquisitions to detect coronary artery disease in obese and nonobese patients. J Nucl Cardiol. 2006;13:191–201.
7. Hayes SW, De Lorenzo A, Hachamovitch R, Dhar SC, Hsu P, Cohen I, et al. Prognostic implications of combined prone and supine acquisitions in patients with equivocal or abnormal supine myocardial perfusion SPECT. J Nucl Med. 2003;44:1633–40.
8. Goto K, Takebayashi H, Kihara Y, Yamane H, Hagikura A, Morimoto Y, et al. Impact of combined supine and prone myocardial perfusion imaging using an ultrafast cardiac gamma camera for detection of inferolateral coronary artery disease. Int J Cardiol. 2014;174:313–7.
9. Nishiyama Y, Miyagawa M, Kawaguchi N, Nakamura M, Kido T, Kurata A, et al. Combined supine and prone myocardial perfusion single-photon emission computed tomography with a cadmium zinc telluride camera for detection of coronary artery disease. Circ J. 2014;78:1169–75.
10. Hindorf C, Oddstig J, Hedeer F, Hansson MJ, Jögi J, Engblom H. Importance of correct patient positioning in myocardial perfusion SPECT when using a CZT camera. J Nucl Cardiol. 2014;21:695–702.
11. Redgate S, Barber DC, Fenner JW, Al-Mohammad A, Taylor JC, Hanney MB, et al. A study to quantify the effect of patient motion and develop methods to detect and correct for motion during myocardial perfusion imaging on a CZT solid-state dedicated cardiac camera. J Nucl Cardiol. 2016;23:514–26.
12. Daou D, Sabbah R, Coaguila C, Boulahdour H. Impact of data-driven cardiac respiratory motion correction on the extent and severity of myocardial perfusion defects with free-breathing CZT SPECT. J Nucl Cardiol. 2018;25:1299–309.
13. Reyes E, Wiener S, Underwood SR, European Council of Nuclear Cardiology. Myocardial perfusion scintigraphy in Europe 2007: a survey of the European Council of Nuclear Cardiology. Eur J Nucl Med Mol Imaging. 2012;39:160–4.
14. Agostini D, Marie P-Y, Ben-Haim S, Rouzet F, Songy B, Cardiovascular Committee of the European Association of Nuclear Medicine (EANM), et al. Performance of cardiac cadmium-zinc-telluride gamma camera imaging in coronary artery disease: a review from the Cardiovascular Committee of the European Association of Nuclear Medicine (EANM). Eur J Nucl Med Mol Imaging. 2016;43:2423–32.
15. Mannting F, Morgan-Mannting MG. Gated SPECT with technetium-99m-sestamibi for assessment of myocardial perfusion abnormalities. J Nucl Med. 1993;34:601–8.
16. Germano G, Erel J, Kiat H, Kavanagh PB, Berman DS. Quantitative LVEF and qualitative regional function from gated thallium-201 perfusion SPECT. J Nucl Med. 1997;38:749–54.
17. Smanio PE, Watson DD, Segalla DL, Vinson EL, Smith WH, Beller GA. Value of gating of technetium-99m sestamibi single-photon emission computed tomographic imaging. J Am Coll Cardiol. 1997;30:1687–92.
18. DePuey EG, Rozanski A. Using gated technetium-99m-sestamibi SPECT to characterize fixed myocardial defects as infarct or artifact. J Nucl Med. 1995;36:952–5.

19. Danias PG, Papaioannou GI, Ahlberg AW, O'Sullivan DM, Mann A, Boden WE, et al. Usefulness of electrocardiographic-gated stress technetium-99m sestamibi single-photon emission computed tomography to differentiate ischemic from nonischemic cardiomyopathy. Am J Cardiol. 2004;94:14–9.
20. Yoda S, Sato Y, Matsumoto N, Tani S, Takayama T, Nishina H, et al. Incremental value of regional wall motion analysis immediately after exercise for the detection of single-vessel coronary artery disease: study by separate acquisition, dual-isotope ECG-gated single-photon emission computed tomography. Circ J. 2005;69:301–5.
21. Fleischmann S, Koepfli P, Namdar M, Wyss CA, Jenni R, Kaufmann PA. Gated (99m)Tc-tetrofosmin SPECT for discriminating infarct from artifact in fixed myocardial perfusion defects. J Nucl Med. 2004;45:754–9.
22. Bailliez A, Lairez O, Merlin C, Piriou N, Legallois D, Blaire T, et al. Left ventricular function assessment using 2 different cadmium-zinc-telluride cameras compared with a γ-camera with cardiofocal collimators: dynamic cardiac phantom study and clinical validation. J Nucl Med. 2016;57:1370–5.
23. Coupez E, Merlin C, Tuyisenge V, Sarry L, Pereira B, Lusson JR, et al. Validation of cadmium-zinc-telluride camera for measurement of left ventricular systolic performance. J Nucl Cardiol. 2018;25:1029–36.
24. Barone-Rochette G, Leclere M, Calizzano A, Vautrin E, Céline G-C, Broisat A, et al. Stress thallium-201/rest technetium-99m sequential dual-isotope high-speed myocardial perfusion imaging validation versus invasive coronary angiography. J Nucl Cardiol. 2015;22:513–22.
25. Cerqueira MD, Weissman NJ, Dilsizian V, Jacobs AK, Kaul S, Laskey WK, et al. Standardized myocardial segmentation and nomenclature for tomographic imaging of the heart. A statement for healthcare professionals from the Cardiac Imaging Committee of the Council on Clinical Cardiology of the American Heart Association. Circulation. 2002;105:539–42.
26. Konno M, Morita K, Adachi I, Ito Y, Kohya T, Kitabatake A, et al. Quantitative analysis of regional wall motion and thickening by quantitative gated SPECT: comparison with visual analysis. Clin Nucl Med. 2001;26:202–7.
27. Pereztol-Valdés O, Candell-Riera J, Santana-Boado C, Angel J, Aguadé-Bruix S, Castell-Conesa J, et al. Correspondence between left ventricular 17 myocardial segments and coronary arteries. Eur Heart J. 2005;26:2637–43.
28. Bailliez A, Blaire T, Mouquet F, Legghe R, Etienne B, Legallois D, et al. Segmental and global left ventricular function assessment using gated SPECT with a semiconductor cadmium zinc telluride (CZT) camera: phantom study and clinical validation vs cardiac magnetic resonance. J Nucl Cardiol. 2014;21:712–22.
29. Cochet H, Bullier E, Gerbaud E, Durieux M, Godbert Y, Lederlin M, et al. Absolute quantification of left ventricular global and regional function at nuclear MPI using ultrafast CZT SPECT: initial validation versus cardiac MR. J Nucl Med. 2013;54:556–63.
30. Giorgetti A, Masci PG, Marras G, Rustamova YK, Gimelli A, Genovesi D, et al. Gated SPECT evaluation of left ventricular function using a CZT camera and a fast low-dose clinical protocol: comparison to cardiac magnetic resonance imaging. Eur J Nucl Med Mol Imaging. 2013;40:1869–75.
31. Rozanski A, Diamond GA, Berman D, Forrester JS, Morris D, Swan HJC. The declining specificity of exercise radionuclide ventriculography. N Engl J Med. 1983;309:518–22.
32. Rozanski A, Berman DS. The efficacy of cardiovascular nuclear medicine exercise studies. Semin Nucl Med. 1987;17:104–20.
33. Berman DS, Kang X, Tamarappoo B, Wolak A, Hayes SW, Nakazato R, et al. Stress thallium-201/rest technetium-99m sequential dual isotope high-speed myocardial perfusion imaging. JACC Cardiovasc Imaging. 2009;2:273–82.